Available online at www.sciencedirect.com

jmr&t
Journal of Materials Research and Technology

journal homepage: www.elsevier.com/locate/jmrt

Original Article

Sensitivity to hydrogen induced cracking, and corrosion performance of an API X65 pipeline steel in H_2S containing environment: influence of heat treatment and its subsequent microstructural changes

S.H. Mousavi Anijdan [a,*], Gh. Arab [b], M. Sabzi [c], M. Sadeghi [d], A.R. Eivani [e], H.R. Jafarian [e]

[a] Department of Materials Engineering, Science and Research Branch, Islamic Azad University, Tehran, Iran
[b] Department of Mechanical Engineering, Yadegar-e-Imam Khomeini (RAH) Shahre-Rey Branch, Islamic Azad University, Tehran, Iran
[c] Young Researchers and Elite Club, Dezful Branch, Islamic Azad University, Dezful, Iran
[d] Department of Mechanical and Structure Engineering and Materials Science, University of Stavanger, Norway
[e] School of Metallurgy and Materials Engineering, Iran University of Science and Technology (IUST), Tehran, Iran

ARTICLE INFO

Article history:
Received 17 February 2021
Accepted 26 July 2021
Available online 31 July 2021

Keywords:
Hydrogen induced crack
Corrosion behavior
API X65 pipeline steel
Heat treatment
Microstructure

ABSTRACT

In this investigation, the effect of microstructural changes and phase equilibria on corrosion behavior and hydrogen induced cracking (HIC) sensitivity of an API X65 pipeline steel was studied. For this purpose, heat treatment was performed at 850 °C, 950 °C, 1050 °C and 1150 °C to engineer the desired microstructure of this pipeline steel. Then, the microstructural evolution was performed by optical microscopy, and Field Emission Scanning Electron Microscopy (FE-SEM) equipped with Energy Dispersive X-Ray Spectroscopy (EDS). Corrosion properties were evaluated in H_2S environment by open circuit potential (OCP), Potentiodynamic polarization and Electrochemical Impedance Spectroscopy (EIS). As well, HIC sensitivity of the API X65 pipeline steel was assessed by hydrogen charging of the cathode and immediately conducting the tensile test. Microscopy analyses showed that the microstructure of the steel is ferritic-pearlitic together with the islands of martensite/austenite constituents. Increasing the heat treatment temperature reduced the amount of pearlite and increased ferrite grain size. It also stabilized the ferrite content. Corrosion results indicated that no active layer was formed on the surface of this pipeline steel. Also, increasing the heat treatment temperature increased the corrosion resistance and reduced sensitivity to micro-galvanic localized corrosion. As well, results suggested that the sensitivity to HIC in the API X65 pipeline was substantially increased with increasing the amount of pearlite and reducing the amount of ferrite; i.e. at lower heat treatment temperature.

* Corresponding author.
E-mail addresses: hashemmousavi@gmail.com, hashemmousavi@srbiau.ac.ir (S.H. Mousavi Anijdan).
https://doi.org/10.1016/j.jmrt.2021.07.118

1. Introduction

Pipeline steels are strategic tools to transfer oil, gas and petrochemical products, and are one of the most viable means of energy transportation in the world nowadays. However, hydrogen cracking in a sour environment is the most important cause of failure for these widely used steels, particularly when employed in H_2S containing media. The life of the pipeline steels is reduced annually due to the nucleation and growth of the hydrogen cracks. Moreover, special attention has been paid to failure of these pipeline steels due to the presence of H_2S gas as well as a high concentration of CO_2gas in the natural gas in the interior wall of the pipelines [1,2]. The diffusion of hydrogen into the metals and alloys can lead to the following damages [3,4]: reduction of formability and fracture strength of the pipeline steels; creation and activation of surface/internal defects; propagation of defects at stress levels much lower than the stresses required for the mechanical failure of the steels; and macroscopic damages resulting from the entrapment of hydrogen in the mechanical interface of the steels.

Hydrogen can enter an engineering product or structure during the various stages of the production of the equipment or even during the service life of the equipment. Also, hydrogen is absorbed in the steel during pickling, electroplating and welding. Later chemical services, where steels are exposed to water corrosion, galvanic corrosion, environment containing high temperature hydrogen or sour environments such as sour gas, sour crude oil and other H_2S containing environment may lead to hydrogen induced cracking (HIC). In fact, hydrogen diffusion is enhanced by cathodic poisons in aqueous solutions. These poisons prevent the formation of atomic/molecule hydrogen compounds on the surface of the steel. While this process is operational, hydrogen atoms are free to diffuse into the groves and intergranular positions of the steel. The poisons include: cyanides, Sulphur, selenium compounds, arsenic, bismuth, phosphor, antimony, iodine tellurium, and H_2S. Among these poisons, H_2S is the most severe of them. Indeed, environments containing moisturized H_2S are the most aggressive ones in which they easily facilitate hydrogen diffusion into the metals and alloys [3–5].

Generally, hydrogen, in various amounts, is produced on the surface of the steel (interface of the fluid and the internal wall of the pipe), due to the occurrence of the corrosion process, particularly when the pipelines are exposed into H_2S containing environments. Subsequently, hydrogen atoms diffuse into the structure of the pipeline steels in the form of a proton. The hydrogen atoms that diffused into the pipeline steels agglomerate in structural defects such as grain boundaries, dislocations, various sulfides like MnS, oxide inclusions and even carbonitrides precipitates [5–7]. On the other hand, the residual stresses of the steels, the occurrence of corrosion and oxidation products of the internal wall of the pipelines could lead to increased hydrogen diffusion rate into the steels. Ultimately, when the amount of hydrogen of the pipeline steels reaches a critical value required for the growth of the hydrogen crack, either under the influence of stress (internal or external) or without the existence of external stress, hydrogen cracks start to grow, leading to the rapid demolition of the pipe [8,9]. Hydrogen diffusion into the metals and alloys causes corrosion, damage, and eventually failure of the metals. The damages caused due to the corrosion and diffusion of hydrogen atoms can be in the form of hydrogen blistering, embrittlement and cracking, ultimately leading to a catastrophic event in various industries. The alloy would be damaged around the crystal defects due to the diffusion of hydrogen atoms into the alloy and the formation of the hydrogen molecule in various locations around such defects. The alloy locally blows up since the hydrogen molecule has very high volume and cannot easily exit from the structure. This is also called hydrogen blistering [9,10]. Hydrogen blisters can penetrate well into the depth of the alloy, show up in the middle of the thick steel plate or close to the weld nuggets in the pipeline steel. In some instances, hydrogen blisters can be connected to each other along the surface of the metal and through the thickness as well, creating layered tearing, direct crack or ledge wise crack. In such circumstances, these type of hydrogen damages is called hydrogen induced cracking or cracking under the influence of hydrogen and stress (SOHIC). And if the hydrogen damage, due to the diffusion of hydrogen atoms into a high strength/high hardness alloy in the H_2S containing environment, and the resultant sulfide corrosion, is coincided with the stress, it is called sulfide stress corrosion (SSC) [11–13]. The HIC is of a very important type of corrosion degradation and damage in the pipeline steels. It is also named as hydrogen delay crack, and crack due to hydrogen. Although, the exact mechanism of HIC in different alloys, especially in acidic environments, is not clearly defined, it is presumed that the diffusion of atomic hydrogen into the pipeline steel leads to a situation where HIC would occur [13,14]. Apparently, the presence of metallurgical and environmental parameters greatly influences corrosion properties of some widely used industrial pieces. Therefore, attempts were made to control the production parameters, and environmental parameters, using coatings etc., so as to optimize the properties of the pipeline steels [15–17].

Bertoncello et al. [16] investigated the effect of thermal spray aluminum coating on the HIC and SCC properties of high strength low alloy steels (HSLAs) in sour environments. Their results showed that applying thermal spray aluminum coating on the HSLAs leads to a reduced sensitivity to HIC and SCC. In another study, Jack et al. [17] assessed the HIC behavior of the API X65 pipeline steel and showed that cracks were detectable in the through the thickness of the pipe after charging hydrogen. As well, the crack growth was the lowest in the [111] direction in the ordered grains. Fragiel et al. [18] studied the effect of microstructure and temperature on the SCC of the API X65 pipeline steel. They showed that an intragranular crack growth prevails in the ferritic-pearlitic microstructure. As well, with increasing the temperature of the H_2S containing environment, some transformation mechanisms of atomic hydrogen to the molecule hydrogen are activated. Ultimately, they showed that an increased crack growth due to the presence of hydrogen is observed with increasing the temperature of the environment.

As the thermomechanical control processing is the common practice to produce microalloyed steels, depending on the rolling condition (strain rate, strain, temperature, final finishing temperature etc), various microstructures including

polygonal ferrite, equiaxed ferrite, acicular ferrite, martensite/austenite (M/A), bainite, ferrite-bainite, and pearlite would form. Usually, depending on the type of heat treatment that is applied on the pipeline steels, pro-eutectoid ferrite, polygonal ferrite, acicular ferrite and equiaxed ferrite are observable in the microstructure [19–21]. It is seen here that corrosion and HIC are the most important parameters influencing the destruction of the pipeline steels. And to the best of the authors' knowledge, no in-depth analysis has been conducted to understand the effect of phase equilibria and heat treatment condition on the corrosion and HIC behavior of the API X65 pipeline steel. Therefore, this research is primarily focused on understanding the effect of microstructural evolution and phase equilibria on the corrosion behavior and sensitivity to HIC of an API X65 pipeline steel in H_2S containing environment. Such a thorough understanding of the corrosion behavior, especially sensitivity to HIC, has not been reported in the literature.

2. Materials and experimental procedure

The steel samples used for this research were taken from an API X65 pipeline steel. Pieces were taken from an actual pipeline steel plate. The chemical composition of the steel pieces was defined by a spark emission spectrometer quantum instrument, made in Germany. Table 1 provides the chemical composition of the steel of this study. It is important to mention that the steel pieces of this research were used in an environment containing H_2S gas to transport a variety of liquids in oil, gas and petrochemical industries. In the next step, soaking heat treatment at 850 °C, 950 °C, 1050 °C and 1150 °C for 2 h was performed on the API X65 pipeline steel samples. Fig. 1 shows a schematic of the heat treatment performed on this steel.

Heat treated samples were subsequently prepared for microstructural studies. For this purpose, heat treated samples were first cut and cold mounted and then polished by different sand papers followed by alumina abrasive papers. 2% Nital solution was used to etch the samples. An optical microscope model Olympuse, made in Japan, was used for microstructural observation. Also, A Filed Emission Scanning Electron Microscope (FE-SEM) model MIRA3TESCAN-XMU, that was equipped with Energy Dispersive X-Ray Spectroscopy (EDS) detector, was used to further analyze the microstructure. Also, to calculate the percentage of pearlite in the samples of this study, the metallography images were analyzed by ImageJ software.

Corrosion behavior was assessed by open circuit potential (OCP), potentiodynamic potential and electrochemical impedance spectroscopy (EIS) techniques in an environment containing H_2S.To perform these tests, specimens with the dimension of 1 cm^2 were taken from the API X65 pipeline steel plate to be connected to the electrolyte. The rest of the samples were coated. The corrosion cell electrolyte was made of 0.5 wt% acetic acid, 5wt% Sodium chloride dissolved in distilled water. It was also saturated with H_2S. One side of the pipeline steel specimen was immersed into the electrolyte and the other side was connected to the instrument. Every sample was first immersed for 1.5 h in the OCP to achieve a stable condition prior to the corrosion evaluation of the steel in an electrolyte containing H_2S. Then, EIS test was performed in the OCP with the amplitude of 10 mV and the frequency range of 10 mHz–100 kHz. Finally, the potentiodynamic polarization test was done in the range of −1000mV to +1000 mV, with respect to the OCP, and with the scan rate of 0.001 V/s. The corrosion tests were done by AMETEK potentiostat instrument model PARSTAT 2273 using a three standard electrodes cell. An Ag/AgCl electrode was used as the reference electrode, a platinum bar was used as the auxiliary, or counting electrode and heat treated steel samples were used as the working electrode. All corrosion tests of this research were performed at 25 °C. Every test was done three times and the average of these three tests was reported as the test results.

The sensitivity to HIC in the pipeline steel was assessed by charging hydrogen gas into the cathode (based on NACE TM0284 standard) and then immediately conducting the tensile test. The electrochemical method was used to create hydrogen embrittlement (HE) in the test samples. For this purpose, an electrochemical cell was prepared with the API X65 pipeline steel connected to its negative pole (cathode). The hydrogen atoms that were produced have moved towards the cathode and diffused in it. Table 2 provides the characteristics of this electrochemical cell. Platinum was used as the anode of such an electrochemical cell. The modified technique of JIS Z3113 was used to assess the amount of diffusible hydrogen into the steel. Additionally, samples were put into glycerin immediately after removing them from the HIC test cell. A water-ice solution was used as the medium to prevent hydrogen atoms from escaping the samples. The amount of diffusible hydrogen was then measured after 48 h. Finally, the tensile test was carried out by an INSTRON tensile tester model 4400 on the hydrogen charged samples. It is also important to mention that to assess the sensitivity to HIC of the heat treated samples, tensile test was done on the non-charged samples. To make sure of the repeatability of the tensile test results, three tests were done for each sample under the two conditions of charged and non-charged. The average of these three tests, together with the standard deviation is reported here. The ASTM E8 standard test method was used for the tensile tests. The strain rate used, up to the point to failure, was 0.5 N/Sec. The fracture surfaces of the tensile test specimens were analyzed by FE-SEM for fractography purposes and to gauge the possibility of hydrogen cracks formation on the surface.

Table 1 – Chemical composition of the steel investigated in this study (wt%).

Element	C	Si	Mn	P	V	Ti	S	Nb	Fe
Amount	0.19	0.39	1.4	0.02	0.06	0.02	0.001	0.03	Balance

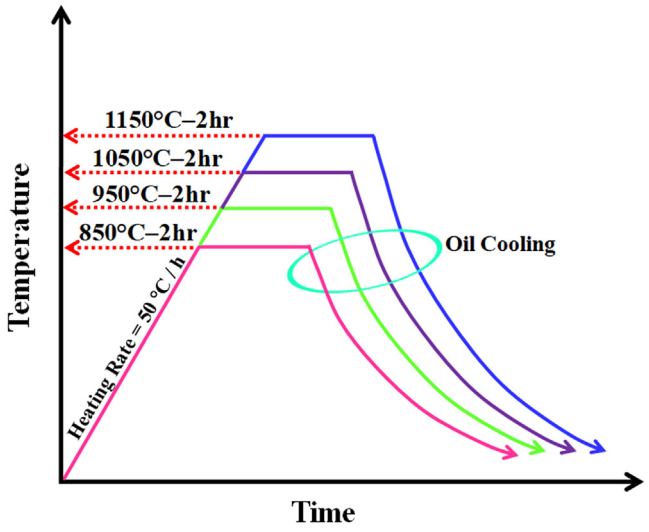

Fig. 1 – Schematic of the heat treatment employed in this study.

3. Results and discussion

3.1. Microstructural evolution

Fig. 2 shows the microstructure of the API X65 steel formed at different heat treatment temperatures. Two phases with the black and white colors can be seen in this figure. The brighter phase is ferrite and the darker one is pearlite. Also, to calculate the percentage of the pearlite phase, the metallography images were analyzed by ImageJ software. The results of this analysis are shown in Fig. 2. The results of ImageJ software shows that the pearlite of the samples heat treated at 850 °C, 950 °C, 1050 °C and 1150 °C were 15.62 ± 0.75%, 12.22 ± 0.47%, 3.91 ± 0.21% and 2.18 ± 0.17%, respectively. Some islands of martensite/austenite can also be seen in the microstructure, which is typical of these microalloyed steels [19,20]. FE-SEM images (with high magnification) together with the EDS analysis was used to better recognize the phases. Fig. 3 shows the results of such analyses. The results indicate that the bright and dark regions are enriched with Fe, hence for the presence of stable phases of ferrite and pearlite in the API X65 pipeline steel. As can be seen in Fig. 2, the steel that is heat treated at 850 °C and 950 °C is fine grained. Such a grain refinement is expected to have a different effect on the corrosion behavior and sensitivity to HIC [22].

Controlling the ferrite grain size, and as a result, strengthening the microalloyed steels is done using the addition of the microalloying elements together with the application of deformation below the no-recrystallization temperature [23–25]. The alloying elements added are usually titanium, vanadium, molybdenum, and niobium which are combined with carbon or nitrogen to form carbides/nitrides or carbonitrides. The Nb carbonitrides usually limit the austenite recrystallization and grain growth during the hot rolling of the microalloyed steels [23]. The resultant ferrite from the pancaked austenite transformation is very fine grained [19–21]. It is clearly seen in Fig. 2 that the amount of pearlite is reduced with increasing the heat treatment temperature. On the other hand, the stability of the ferrite phase and the ferrite grain size has increased. In a sense, with increasing the heat treatment temperature from 850 °C to 1150 °C, the highest amount of ferrite and the lowest amount of pearlite were attained. In fact, the results of this study are well-matched with the results of Godefroid et al. [26], who identified the phases in the pipeline steels in the same way as this research.

Table 2 – The parameters considered for the hydrogen charged cathode of this study.

Parameter	pH	Duration (hours)	Charging current (A/m^2)	Temperature (^0C)
Value	2.7	96	200 ± 5	25 ± 3

3.2. Open circuit potential (OCP)

A voltage is created at the interface of the pipeline steel-electrolyte when the steel is immersed in an H_2S containing electrolyte. This is due to the nature of the electrochemistry of the corrosion process in the pipeline steels. Therefore, it is important to measure such a potential, i.e. open circuit potential. OCP is a potential where electrochemical reactions reach an equilibrium state. It is the pipeline potential under the condition of applying no external current or potential. Enough time should be given to the electrochemical cell prior to the corrosion experiments to achieve this equilibrium in the electrochemical reactions. A stable condition without much fluctuation of the potential is acquired under this circumstance. In fact, such a stable condition is obtained after a few minutes in some cells and after a few hours in others [27,28]. Usually, the corrosion current density is predictable based on the OCP. For this reason, first of all, OCP of the pipeline steel in the electrolyte is designed to make sure of the steel surface stability in the desired environment. Other corrosion tests are conducted based on the OCP of the pipeline steel in the H_2S environment. The variation of potential versus time was recorded for the API X65 pipeline steel immersed in the designed electrolyte. Depending on the chemical composition of the steel, microstructure and corrosion resistance of the steel, a certain time is needed for the oxide layer to form on the surface of the steel and to transform it an electrical double layer. Thus, the variation of the OCP of pipeline steel during the immersion time is highly dependent on the mentioned parameters. Even the time to reach a constant value during the OCP test can be predicated on the microstructural evolution and phase equilibrium of the pipeline steel, i.e. the metallurgical effect on corrosion resistant [29,30].

In Fig. 4 the variation of potential versus immersion time (OCP) is shown for the API X65 pipeline steel at different temperatures. Region one of the OCP curves starts at about the starting time of immersion up until 20 min after immersion. It is seen in this figure that, in such a condition, the voltage is rapidly decreasing linearly for all four heat treated samples. This phenomenon shows that no oxide film has started to form on the surface of the API X65 pipeline steel. With increasing the immersion time, the fluctuation of the potential decreases in a way that the lowest value of potential

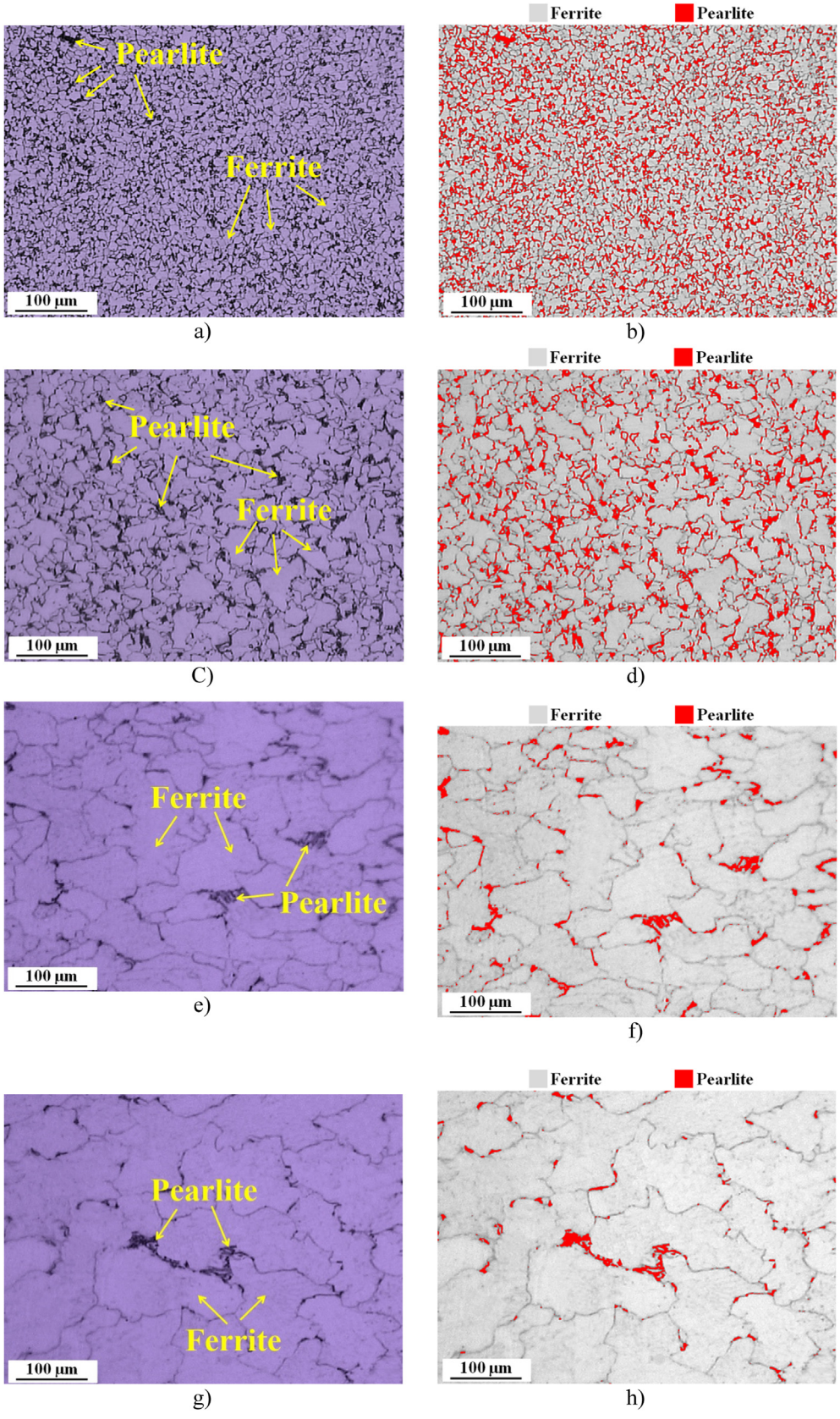

Fig. 2 – Optical micrographs and ImageJ analyses for the pipeline steel samples heat treated at different temperatures: a,b) 850 °C, c,d) 950 °C, e,f) 1050 °C, g,h) 1150 °C.

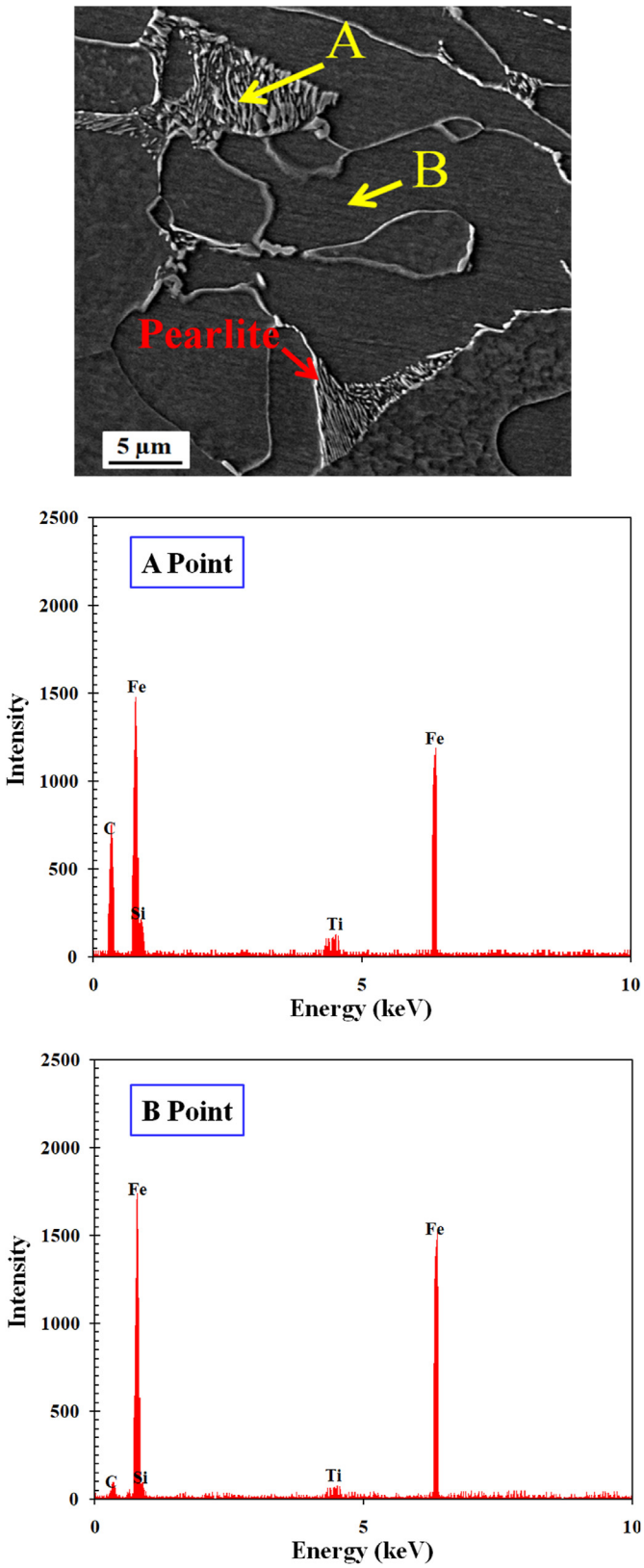

Fig. 3 – FE-SEM micrograph together with the EDS analysis of the points mentioned in the micrograph of the sample heat treated at 850 °C.

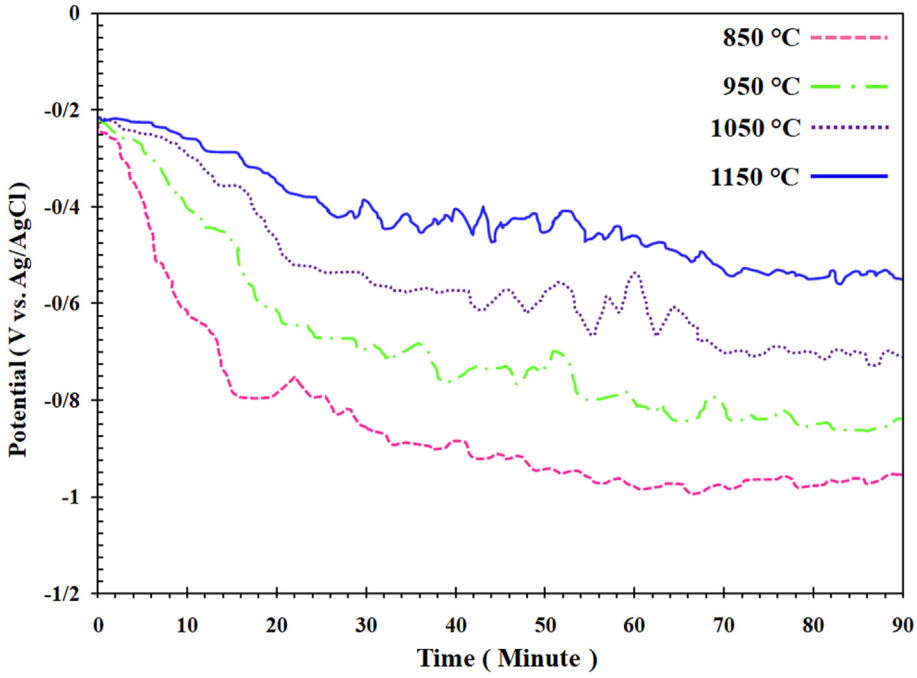

Fig. 4 – The effect of heat treatment temperature on the OCP curves for the API X65 pipeline steel in a H_2S containing environment.

fluctuation for the OCP is observed after about 70 min of immersion. As can be also seen in the OCP curves, with decreasing the heat treatment temperature, the OCP shifted towards very negative values. This is indicative of the higher activity of the pipeline steel immersed in the H_2Scontaining environment. In fact, this condition is suggestive of the effect of reducing the heat treatment temperature, and as a result increasing the amount of pearlite, on the excitation of the pipeline steel in terms of corrosion susceptibility in the H_2S environment. In a sense, this phenomenon is distinguished in the OCP curves in changing the potential of the surface of the steel towards more negative values. The main reason is the very different electrochemical behavior of the pearlite and ferrite phases of the microstructure of the steel. Indeed, a

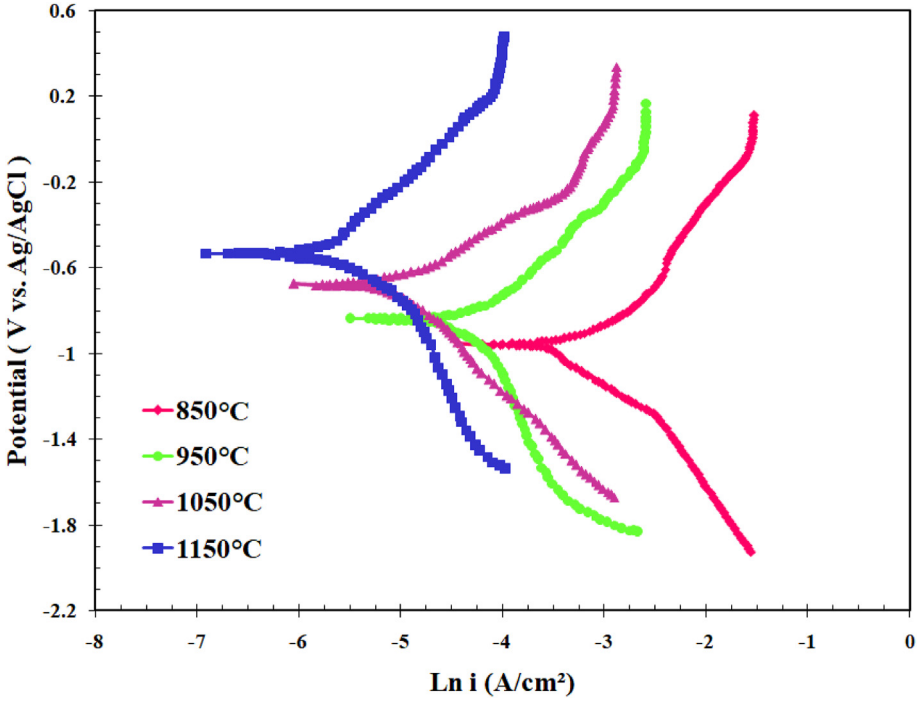

Fig. 5 – Polarization curves obtained from the potentiodynamic polarization test for the API 65 pipeline steel.

Table 3 – Electrochemical parameters extracted from the potentiodynamic polarization test of Fig. 5.

Sample treated at the temperature (°C)	850	950	1050	1150
E_{corr} (mV vs. Ag/AgCl)	−963± 9	−836± 7	−688± 9	−533± 8
I_{corr} (μA/cm^2)	35,936± 9	14,552 ± 7	7041 ± 8	4091± 9
Corr. Rate (mm/year)	1.27 ± 0.12	0.91 ± 0.10	0.78 ± 0.09	0.35 ± 0.07

micro galvanic peel is formed and corrosion reaction is intensified on the surface of the steel due to the higher reaction tendency of the pearlite, and lower reaction tendency of ferrite, inside the corrosion cell [31].

3.3. *Potentiodynamic polarization*

Fig. 5 shows the potentiodynamic polarization curves of the steel in H_2S containing environment at different temperatures. As well, the electrochemical parameters extracted from these potentiodynamic polarization curves are provided in Table 3. It is important to mention that the possibility of measuring very low rates of corrosion is remote for the pipeline steel in the Tafel extrapolation technique. Such corrosion rates can be deduced from the intersection of the linear portion of the Tafel curves [32,33]. Electrochemical parameters such as corrosion potential (E_{corr}), corrosion current density (I_{corr}) and polarization resistance or resistance against corrosion (R_p) were calculated from the extrapolation of the Tafel curves (Fig. 5) for the API X65 pipeline steel. The results of the potentiodynamic polarization test show that with increasing the heat treatment temperature, the corrosion resistance increases and corrosion current density decreases. It is also seen in the curves of Fig. 6 that current density was reduced in both anodic and cathodic branches as the amount of pearlite phase reduced. This is indicative of the effect of microstructural changes and phase equilibrium on both the cathodic and anodic corrosion reaction of the steel in the H_2S environment. There are two plausible reasons for this phenomenon:

a) The grain boundaries area increases with the reduction of ferrite grains at lower heat treatment temperatures. And since grain boundaries are high energy regions which increase the tendency for corrosion reactions, such an increase in the area increases the current density and corrosion rate as such.
b) Pearlite and ferrite phases show two different electrochemical behaviors. The number of micro-galvanic peel increases with increasing the amount of pearlite at lower heat treatment temperature. Therefore, as the amount of pearlite in the phase equilibrium increases, the susceptibility for the micro-galvanic localization corrosion increases.

Overall, the results reduced from the potentiodynamic polarization test are well matched with the results of the OCP test. It is obvious from both tests that the corrosion resistant of the steel was substantially reduced with increasing the amount of pearlite and the reduction of ferrite grain size; i.e. lower heat treatment temperature. In a sense, the corrosion potential of the pipeline steel moved towards very negative values under such a scenario.

3.4. *Electrochemical impedance spectroscopy (EIS)*

The Nyquist curves together with the Bode and Bode-Phase curves resulting from the EIS test for the pipeline steel of this study is shown in Fig. 6. The EIS test was conducted to assess the reactions on the interface of steel/electrolyte, and also to evaluate the reactions on the surface of the steel in the H_2S environment. The results of Fig. 6 show that all samples have a single impedance resistance ring and no sign of passive layer is observed on the surface of the steel. In fact, it is seen in the EIS test results that the diameter of the Nyquist plots was substantially increased with increasing the heat treatment temperature (increasing the diameter of the ferrite grains and reducing the amount of pearlite). This is indicative of the effect of ferrite grain boundaries, and reducing pearlite in the microstructure, on the corrosion response of the steel surface in the H_2S environment. In fact, the Nyquist curves obtained from this study were in the form of a defected half circle. Such a half circle Nyquist curves of Fig. 7a could be due to the surface irregularity. They could also be due to the control of the corrosion response by the charge transfer on the surface of the API X65 pipeline steel [34,35]. This is suggestive of the fact that the corrosion resistance of the steel increases with increasing the heat treatment temperature in a way that proper compatibility is observed between the OCP, potentiodynamic polarization, and Nyquist curves.

The results of EIS tests in the form of Bode and Bode-Phase curves are shown in Figs 6b and c, respectively. Commonly, the Bode curves should be linear with the slope of minus one for the pipeline steel, which provides acceptable protection properties. However, the slope of the Bode curve changes with the hydrogen atoms/molecules attack as well as the diffusion of the corrosive ions such as Cl^-/oxygen into the surface layer of the pipeline steels. With such an attack, the corrosion starts at the interface of the H_2Scontaining electrolyte and the pipeline. Therefore, the protective behavior of pipeline steel in an environment containing H_2S can be assessed by the deviation of the slope of the Bode curves from the negative value, and by their comparison with the Nyquist plots [36,37].

In Fig. 6b the effect of heat treatment temperature on the Bode curves of the API X65 pipeline steel is shown. The following remarks can be made from the curves:

1 All the Bode curves for the heat treated API X65 pipeline steel at different temperatures contain a negative slope. The presence of only one negative slope in these curves is indicative of the fact that only on impedance ring or one constant phase element is formed in the impedance response of this pipeline steel [38,39]. In a sense, the Bode curves presented in Fig. 6b endorse the results of the Nyquist plots and the fact that no passive layer was formed on the surface of the API X65 steel.

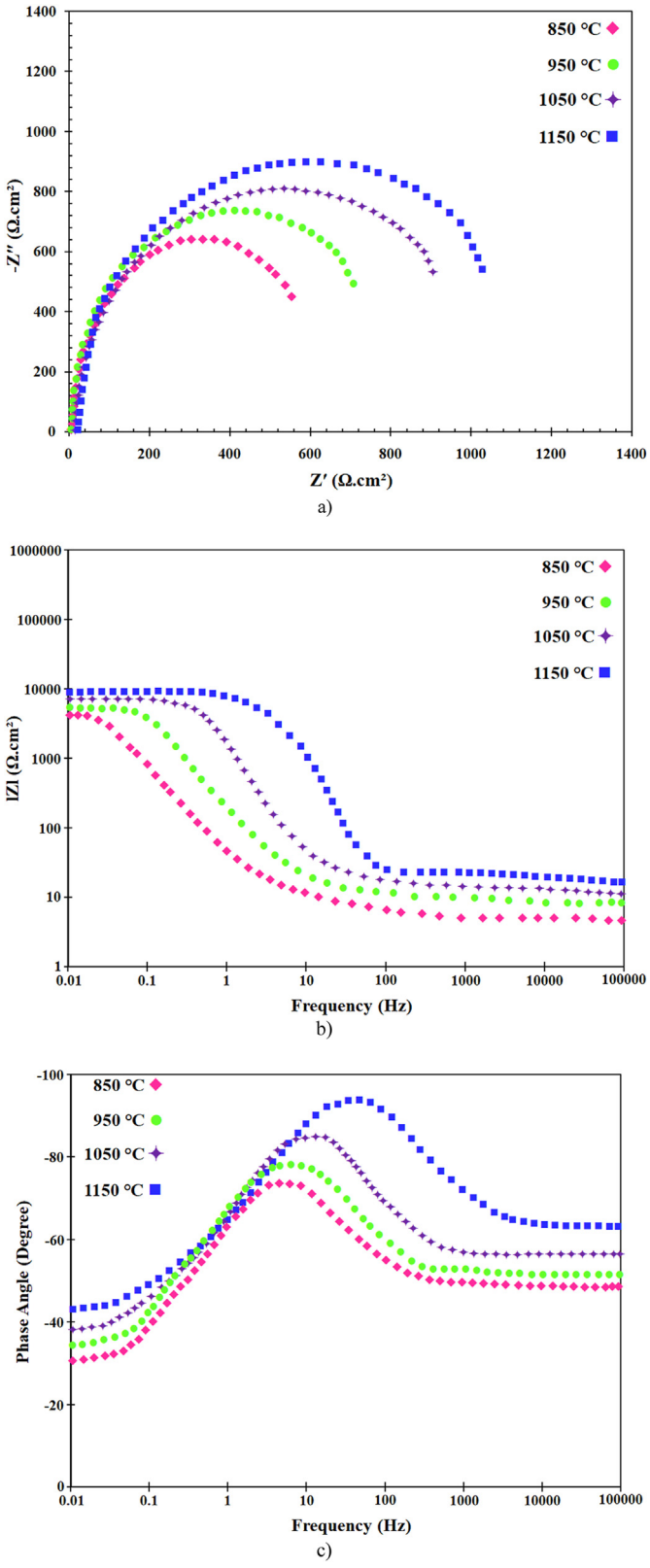

Fig. 6 – The results of EIS tests for the API X65 pipeline steel in an H_2S containing environment, a) Nyquist curves, b) Bode curves, c) Bode-Phase curves.

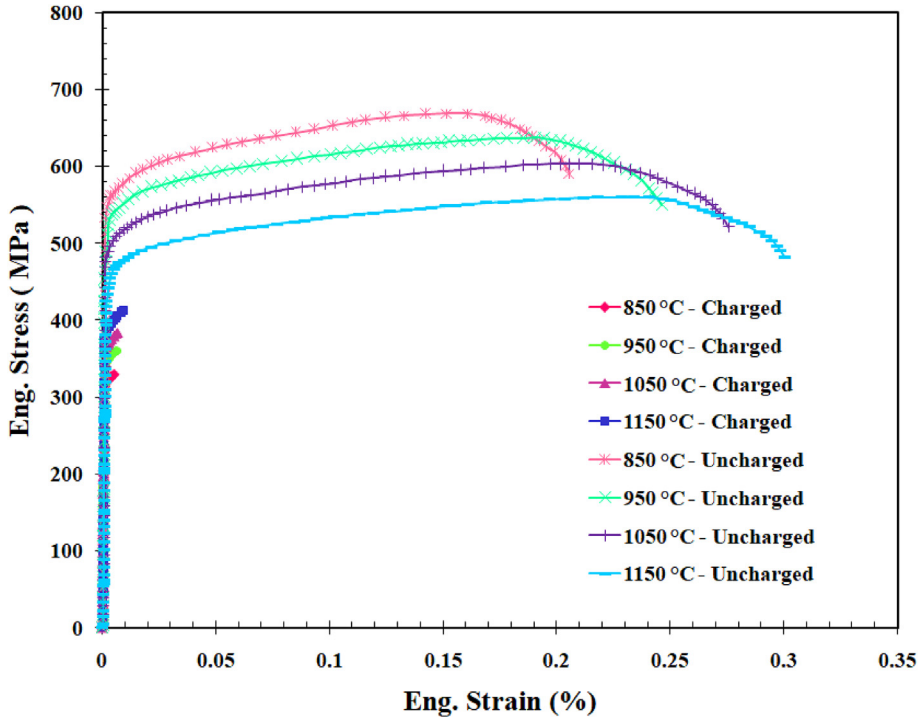

Fig. 7 – Stress–strain curves for the hydrogen charged and non-charged samples of the pipeline steel.

2 It can be observed in the Bode curves that increasing the heat treatment temperature, which reduces pearlite and increases the stability of the ferrite, increases the impedance resistance of the pipeline steel. In fact, similar to the Nyquist curves, the Bode curves are suggesting that increasing the heat treatment temperature enhances the corrosion resistance of the steel in the H_2S containing environment.

The Bode-Phase curves are depicted in Fig. 6c. It can be clearly seen in the Bode-Phase curves of the heat treated steel that only one peak exists. This confirms that only one constant phase element is present in the impedance result of the API X65 pipeline steel at each temperature. It is also seen in these curves that the highest peak corresponds for the sample that was heat treated at 1150 °C. In a sense, the higher the peak height of the Bode-Phase curve, the higher the corrosion resistance of the steel, and the better the protection properties created in the API X65 pipeline steel [38,39]. In fact, the highest peak is seen in the range of −70 °C to −90 °C for the sample heat treated at 1150 °C. Overall, the results of the EIS tests, in the form of Nyquist plots, Bode curves and Bode-Phase curves are compatible with one another. They are also well matched with the results of Bordbar et al. [31], who reported that the corrosion resistance of an API X70 steel increases as the amount of ferrite increases in its microstructure.

3.5. *Sensitivity to HIC*

The amount of diffusible hydrogen atoms into the API X65 pipeline steel was assessed based on the modified JIS Z3113 method. Table 4 provides the results of such analysis. The tensile test was also performed on the charged samples after hydrogen charging of the cathode. The stress–strain curves result of this test is shown in Fig. 7. As well, the fracture surfaces of the tensile test specimens were analyzed by FE-SEM, the results of which are depicted in Fig. 8. It can be observed from Table 4 that, with increasing the amount of pearlite and reducing ferrite packet size (through reducing the heat treatment temperature), the highest amount of diffused hydrogen followed in the sample heat treated at 850 °C. On the other hand, the amount of pearlite was reduced, and the ferrite grain size increased with increasing the heat treatment temperature. On the other hand, the amount of hydrogen atoms diffused into the pipeline steel was reduced as such. This phenomenon is due to the decreased amount of grain boundaries areas. Such areas are the preferential locations for the entrapment of the hydrogen atoms. Additionally, it is well known that pearlite itself consists of lamellar morphology of cementite and ferrite. The free spaces within this lamellar morphology (between layers) can be favorable locations for the diffusion and entrapment of the hydrogen atoms/molecules in the heat treated samples.

Moreover, it can be observed in Table 4 that hydrogen diffused in the steel is at almost the saturated level (about 4–5 ppm). This amount of hydrogen is relatively high for the pipeline steels. It can be deduced from this analysis that most

Table 4 – The amount of diffused hydrogen in different heat treated steel samples.

Heat treatment temperature (°C)	850	950	1050	1150
Diffused hydrogen (ppm)	5.3 ± 0.1	4.8 ± 0.1	4.4 ± 0.1	3.8 ± 0.1

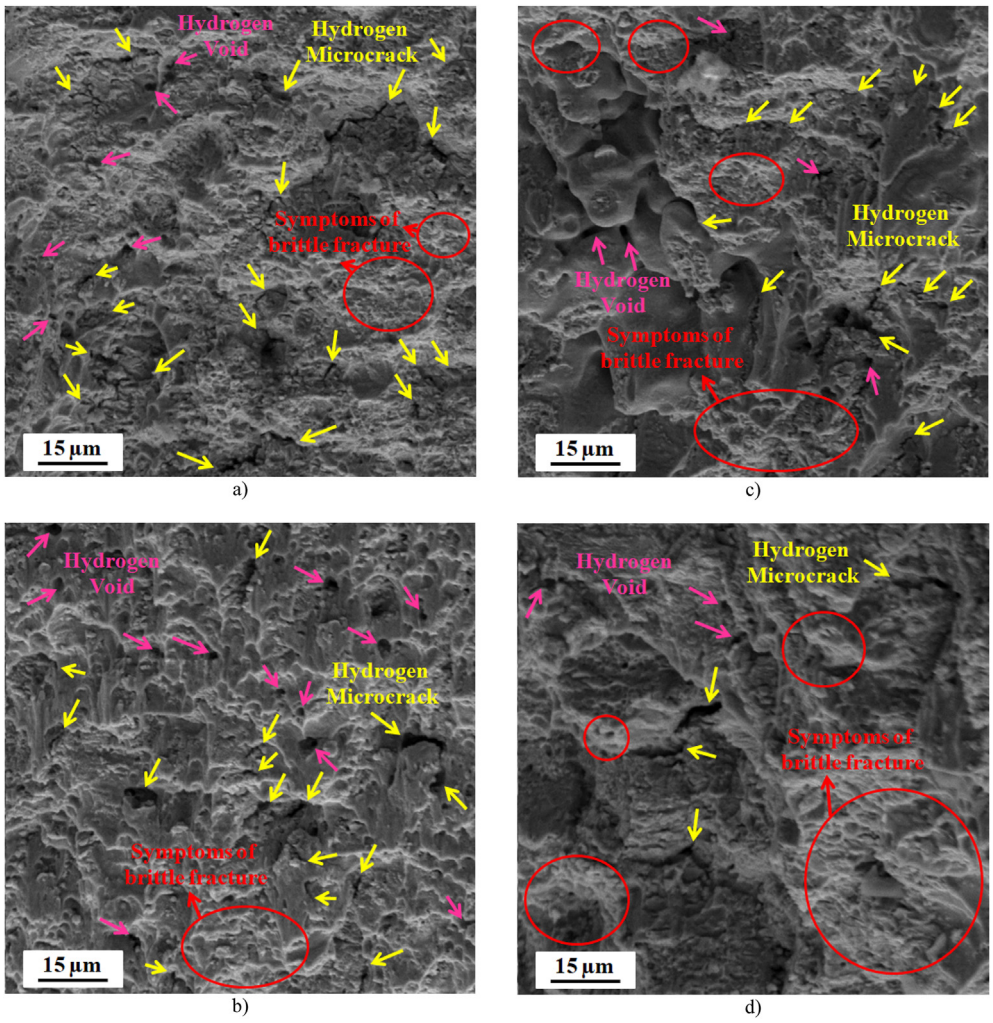

Fig. 8 – FE-SEM micrographs on the fractured tensile samples heat treated at different temperatures (charged condition), a) 850 °C, b) 950 °C, c) 1050 °C, d) 1150 °C.

of the dislocations are surrounded by hydrogen atoms and their movement within the crystal structure of the steel is very limited. This was due to the fact micro-cracks are formed in the crystal structure when the agglomeration of the hydrogen atoms/molecule is increased in the pipeline steel. In fact, the formation and the growth of the micro-crack were much faster than the dislocation pinning by the hydrogen atoms, hence for this to be the dominant mechanism.

Fig. 7 and Table 5 show the results of the tensile tests, together with the standard deviations, that were performed on the hydrogen charged and non-charged samples. These results clearly show that the sensitivity to HIC was significantly increased at the presence of hydrogen, increasing the trapped hydrogen and increasing the diffusion of hydrogen into the structure of the pipeline steel. In fact, the strength and elongation percentage were substantially reduced with increasing the trapped hydrogen and the hydrogen diffusion as well. In the hydrogen charged samples, the highest sensitivity to HIC was related to the sample heat treated at 850 °C. Under the hydrogen charged condition, this sample showed yield strength of ~325 MPa and percentage elongation of 0.0067%. This is while, under the non-charged condition, the yield strength of this sample was ~574 and its elongation percentage was 0.2059%. On the other hand, it is seen in the tensile test results that the lowest sensitivity to HIC in the charged samples is for the sample heat treated at 1150 °C. Under the hydrogen charged condition, this sample showed yield strength of ~407 MPa and elongation percentage of 0.0117%. This is while, under the non-charged condition, the yield strength of this sample was ~481 MPa and its percentage elongation was 0.3003%. The reason for this phenomenon is, as observed in the metallographic analysis, the increased ferrite grain size and the reduced pearlite percentage by increasing the heat treatment temperature from 850 °C to 1150 °C. Therefore, under the condition of non-charged hydrogen, the sample heat treated at 850 °C has the highest yield strength and the lowest elongation percentage due to its small ferrite grain size and high elongation percentage. In a sense, the grain boundaries act as a barrier for the movement of dislocations and lead to dislocation pile up, hence for the increased strength. And due to the presence of this low amount of grain boundaries and lower pearlite in the

Table 5 – Results obtained from tensile test for the hydrogen charged and non-charged samples.

Sample	Yield Strength (MPa)	Tensile Strength (MPa)	Elongation at Break (%)
850°C-Charged	325 ± 6	–	0.0067 ± 0.0005
950°C-Charged	359 ± 8	–	0.0077 ± 0.0005
1050°C-Charged	379 ± 7	–	0.0083 ± 0.0007
1150°C-Charged	407 ± 6	–	0.0117 ± 0.0011
850°C-non-charged	574 ± 8	668 ± 9	0.2059 ± 0.0019
950°C- non-charged	548 ± 7	637 ± 6	0.2458 ± 0.0017
1050°C- non-charged	511 ± 8	603 ± 7	0.2757 ± 0.0016
1150°C- non-charged	481 ± 8	560 ± 8	0.3003 ± 0.0014

hydrogen charged sample heat treated at 1150 °C, this sample shows the highest yield strength. Overall, the yield strength and elongation percentage obtained in Table 5 are compatible with the amount of diffused hydrogen into the different samples of this study. In fact, the presence of hydrogen, increased hydrogen trapping and also increased hydrogen diffusion into the microstructure lead to the reduction of yield strength in the API X65 pipeline steel. Therefore, it can be concluded that the strength and plastic deformability of the sample was reduced by diffusing hydrogen into the API X65 pipeline steel. On the other hand, it can be said that a higher amount of hydrogen was entrapped in the steel microstructure with reducing the heat treatment temperature. In a sense, such hydrogen entrapment increased internal stress of the steel causing an earlier fracture.

The fracture surfaces of the tensile test specimens were analyzed by FE-SEM technique to characterize hydrogen cracking and to define the fracture mode. Fig. 8 shows the results of this analysis. It is visibly seen in the fracture surfaces of different samples that all hydrogen charged samples were broken by a completely brittle fracture mode. This fracture morphology was predicted from the very small plastic strain observed in the stress–strain curves of the samples in Fig. 7. Commonly, a soft fracture with dimple characteristic is envisaged if the steel is ferritic and free of hydrogen as well. However, since the hydrogen atoms/molecules that cause HIC phenomenon have diffused into the APIX65 pipeline steel structure, the condition was suitable for the nucleation and growth of the hydrogen crack during the tensile stress. It is important to note that, due to the presence of different amounts of pearlite and grain boundaries, the concentration of hydrogen is not the same throughout the sample. Therefore, the concentration of hydrogen increases, after applying tensile stress, in the areas of the structure that contain pearlite and grain boundaries. The continuous increment of hydrogen concentration in these preferential locations leads to the creation of micro-cracks in the microstructure. Eventually, the growth and coalescence of these micro-cracks during the application of tensile stress cause earlier fracture of the pipeline steel [40,41].

The theory of the interaction of hydrogen and dislocations was first proposed by Morton and Vaughan in 1956. This damage mechanism is explained by the formation of Cottrell atmosphere around the dislocations. Based on this theory, the interaction of some hydrogen atoms with the dislocations in the crystal leads to the reduction of dislocations motion and as result creates microscopic work hardening [42,43]. This phenomenon lowers and even eliminates plastic deformability in steels. Among the different microstructures of the pipeline steels, the pearlitic microstructure is more prone to the hydrogen cracks compared to the ferritic one due to its higher hardness and more brittleness. Hydrogen atoms are agglomerated in the free spaces between the pearlite layers, ferrite grain boundaries, or in the free space between the inclusions and the matrix. Therefore, when hydrogen atoms are trapped in these locations and are transformed into atomic/molecule gas, they cause hydrogen cracking due to the exertion of very high pressure in those regions. This phenomenon is shown in Fig. 9. In fact, it can be deduced from Fig. 9 that the hydrogen induced crack advances where a higher percentage of pearlite exists, or where a high percentage of grain boundaries exist in the microstructure. This is due to the fact that pearlite, as a hard phase, provides a higher possibility for the easier advancement of the hydrogen induced crack. Moreover, since the pearlite structure itself consists of two phases of ferrite and cementite, the free spaces between the layers of these two phases can act as the preferential locations for the entrapment of hydrogen atoms/molecules. Hence, for the increased sensitivity to HIC of the pipeline steel.

The pipeline steel carrying crude oil or natural gas is often used in acidic environments containing H_2S. When the corrosion conditions are provided, particularly at the presence of moisture, such H_2S containing environments cause severe corrosion on the surface of the steels [44,45]. During such corrosion reactions and the damages that the corrosive agents create on the surface of the pipeline steels, hydrogen atoms can move freely inside the electrolyte (environment). Ultimately, these hydrogen atoms can be agglomerated locally on the surface of the steel. Subsequently, over time, these hydrogen atoms can diffuse into the steel structure based on what is shown in Fig. 8. In fact, the reactions that occur for the pipeline steel in the H_2S containing environments, which leads to hydrogen damage, as follows:

$$H_2S \rightarrow 2H^+ + S^{2-} \quad (1)$$

$$Fe + 2H^+ \rightarrow Fe^{2+} + 2H \quad (2)$$

$$Fe^{2+} + S^{2-} \rightarrow FeS \quad (3)$$

$$H_2S + Fe \rightarrow FeS + 2H \quad (4)$$

On the other hand, the diffusion of hydrogen atoms into the crystal structure of the API X65 pipeline steel occurs in three steps. In the first stage, physical adsorption is happening. During this stage, van der Waals forces act on the interface and produce atomic absorption. In the second stage, chemical absorption is happening, where a chemical reaction occurs between the atoms on the surface of the pipeline steel and the absorber. In the third and final stage, the diffusion of the hydrogen atoms is happening. In this last stage, the products of the second stage diffuse into the crystal structure of the pipeline steel. The hydrogen atoms diffused into the crystal structure of the steel agglomerate in structural defects such as grain

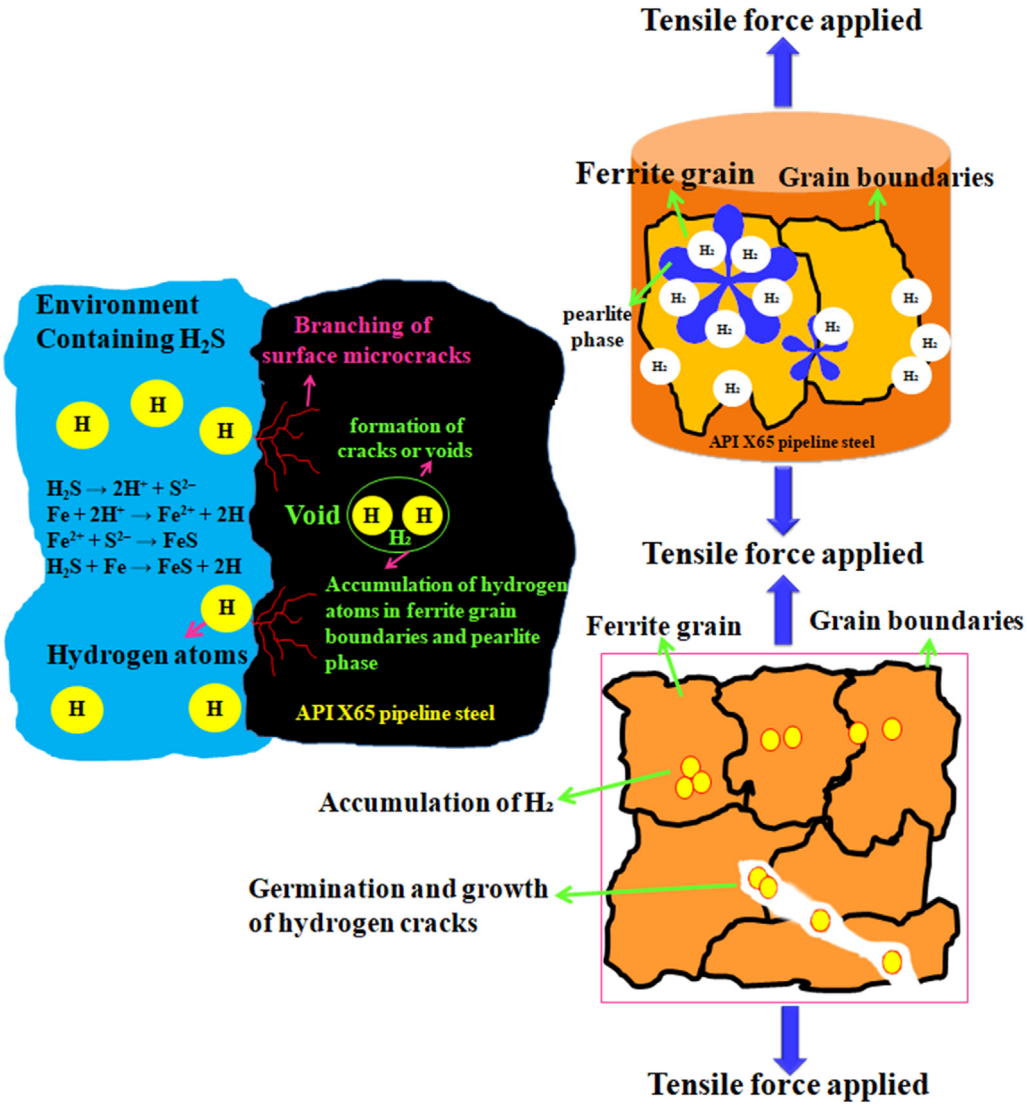

Fig. 9 – Various steps of hydrogen diffusion into the microstructure of the pipeline steel and the formation of hydrogen crack in the crystal structure.

boundaries, inclusions, segregation locations of the alloying elements, dislocations, solidification cracks or micro-voids. They combine with each other in these locations and create hydrogen molecules gas or hydrogen damage. This process produces a substantial amount of pressure. When such pressure exceeds the yield strength of the API X65 pipeline steel, hydrogen crack starts to form in the crystal structure. As explained above, in the first stage the diffusion of hydrogen atoms into the crystal structure is occurring. Such atoms get agglomerated in the grain boundaries and the pearlite layers. In the next step, the hydrogen atoms are combined and create hydrogen molecules. Such a transformation coincides with increased pressure and the microstructure of the steel experiences stress level higher than its yield strength. Ultimately, the nucleation and growth of the hydrogen crack are due to the exerted pressure resulting from the changes of the hydrogen atoms to the hydrogen molecules.

Several hypotheses were proposed for the nucleation and growth of the HIC crack. However, a theory proposed by Zapffi and Tetelman [46,47], regarding the nucleation and growth of hydrogen crack in the HIC process, has gained widespread acceptance among the many theories in the field. This hypothesis is known as the internal pressure theory and is one of the most acceptable explanations concerning HIC. Based on this theory, hydrogen atoms agglomerate on structural defects such as MnS inclusions, oxide compounds inclusions, carbides, nitrides, and on phases such as pearlite (lamellae) in the dominant matrix phase of the alloys. Then, hydrogen cracks nucleate and growth when the hydrogen pressure, resulting from the transformation of hydrogen atoms to hydrogen molecules, increases. This process is schematically explained in Fig. 9. In this figure, the diffusion and absorption mechanism of hydrogen into the microstructure of the pipeline steel, together with the different preferential locations for the entrapment of

hydrogen atoms are shown. As well, the process of increased hydrogen pressure in structural defects is depicted.

4. Conclusions

In this study, the effect of microstructural changes and phase equilibria on the corrosion behavior and sensitivity to HIC were evaluated in an API X65 pipeline steel. Various heat treatment processes were applied to such steel to acquire different microstructure and a combination of phases. Various microscopic, and corrosion evaluation tests were employed under the exposure of H_2S gas. HIC sensitivity was assessed by charging hydrogen to the cathode and then immediately performing tensile tests. The following conclusions were drawn from this research:

a Microstructural observation showed that the steel structure is mostly ferritic-pearlitic, together with the M/A islands, in a way that ferrite was the matrix. Increasing the temperature deduced ferrite and increased ferrite grain size and its stability.

b The results of ImageJ software analysis showed that increasing the heat treatment temperature from 850 °C to 1150 °C led to the reduction of pearlite in the steel structure from 15.62 ± 0.75% to 2.18 ± 0.17%.

c Assessing OCP curves showed that by reducing the heat treatment temperature (increasing pearlite and the grain boundary areas of ferrite), OCP moved towards very negative values. This is indicative of the higher activity of the API X65 steel immersed in the H_2S containing environment. Also, potential fluctuation in the OCP curves followed a downward trend during the whole 1.5 h of immersion which was suggestive of the absence of a passive layer on the steel surface.

d Potentiodynamic polarization curves showed that corrosion resistance increased and corrosion current density reduced with increasing the heat treatment temperature. The current density was reduced in both the cathodic and the anodic branches of the Tafel with increasing the ferrite grain size and decreasing pearlite. This phenomenon confirmed the effect of microstructural evolution and its subsequent phase change on both the cathodic and anodic corrosion of the API X65 steel.

e EIS results showed that with increasing the heat treatment temperature, the diameter of the Nyquist curves was substantially increased. Bode-Phase curves of the heat treated steel had the same negative slope at different temperatures. These curves also showed only one peak. The highest peak was in the range of −70° to −90° for the sample heat treated at 1150 °C.

f The highest amount of hydrogen was diffused and trapped in the sample as the amount of pearlite increased and ferrite grain size reduced (at lower heat treatment temperature). Such a condition occurred at 850 °C.

g It was seen in the tensile test results of the hydrogen charged sample that the sensitivity to HIC of the pipeline steel was increased with increasing the amount of trapped hydrogen and with the increasing the diffusion of hydrogen into the structure. This has resulted in a significant reduction of strength and elongation percentage. The highest sensitivity to HIC occurred in the charged samples heat treated at 850 °C. This was while such a sample showed the highest strength and elongation percentage under the non-charged condition.

h Fractography analysis of the tensile test samples showed that ductility was almost non-existent by the diffusion of hydrogen into the microstructure of the API X65 pipeline steel, leading to the occurrence of brittle fracture. All fracture surfaces contained micro-cracks indicative of the hydrogen induced cracking on the surface. Increasing the amount of pearlite and reducing ferrite substantially increased HIC sensitivity in the steel.

Data availability statement

The raw/processed data required to reproduce these findings cannot be shared at this time as the data also forms part of an ongoing study.

Declaration of Competing Interest

The authors declare that they have no known competing financial interests or personal relationships that could have appeared to influence the work reported in this paper.

REFERENCES

[1] Moon J, et al. Influence of precipitation behavior on mechanical properties and hydrogen induced cracking during tempering of hot-rolled API steel for tubing. Mater Sci Eng, A 2016;652:120–6.

[2] Li L, Song B, Cui Xi, Liu Zh, Wang L, Cheng W. Effects of finish rolling deformation on hydrogen-induced cracking and hydrogen-induced ductility loss of high-vanadium TMCP X80 pipeline steel. Int J Hydrogen Energy 6 2020;45(55):30828–44.

[3] Singh Vishal, Singh R, Arora K Singh, Mahajan DK. Hydrogen induced blister cracking and mechanical failure in X65 pipeline steels. Int J Hydrogen Energy 2019;44:22039–49.

[4] Gong K, Wu M, Xie F, Liu G, Sun D. Effect of dry/wet ratio and pH on the stresscorrosion cracking behavior of rusted X100 steel in an alternating dry/wet environment. Construct Build Mater 2020;260:1–9.

[5] Santos BAF, Souza RC, Serenario MED, Gonçalves MC, Mendes Júnior EP, Simões TA, et al. The effect ofdifferent brines and temperatures on the competitive degradation mechanisms of CO_2 and H_2 Sin API X65 carbon steel. J Nat Gas Sci Eng 2020;80:1–13.

[6] Li J, Gao Xi, Du L, Liu Zh. Relationship between microstructure and hydrogen induced cracking behavior in a low alloy pipeline steel. J Mater Sci Technol 2017;33(Issue 12):1504–12.

[7] Shi Xi, et al. Novel Cu-bearing high-strength pipeline steels with excellent resistance to hydrogen-induced cracking. Mater Des 2016;92:300–5.

[8] Zhang D, Gao Xi, Du Yu, Du L, Wang H, Liu Zh, et al. Effect of microstructurerefinement on hydrogen-induced damage behavior of low alloy high strength steel for flexibleriser. Mater Sci Eng, A 2019;765:1–10.

[9] Poorhaydari K. Failure of a hydrogenerator reactor inlet piping by high-temperature hydrogen attack. Eng Fail Anal 2019;105:321–36.
[10] Li Sh, et al. Influence of surface martensite layer on hydrogen embrittlement of Fe-Mn-C-Mo steels in wet H2S environment. Int J Hydrogen Energy 2018;43(Issue 34):16728. 1673.
[11] Li Xi, et al. Effect of surface roughness on hydrogen-induced blister behavior in pure iron. Metals 2020;ume745:1–14.
[12] Wang Q, Sun Y, Shi G, Meng K, Wang Qi, Zhang F. Effect of niobium on sulfidestress cracking behavior of tempered martensitic steel. Corrosion Sci 2020;165:1–12.30. In press.
[13] Shi Xi, et al. HIC and SSC behavior of high-strength pipeline steels. Acta Metall Sin 2015;28:799–808.
[14] Yoon B. Characteristics of sulfide stress cracking of high strength pipeline steel weld by heat input. Journal of Welding and Joining 2018;36:38–44.
[15] Lavvafi H, Lewandowski ME, Schwam D, Lewandowski JJ. Effects of surface laser treatments on microstructure, tension, and fatigue behavior of AISI 316LVM biomedical wires. Mater Sci Eng, A 2017;688:101–13.
[16] Bertoncello JCB, Simoni L, Tagliari MR, Scheid A, Paes MTP, Kwietniewski CEF. Effects of thermal spray aluminium coating on SSC and HIC resistance of high strength steel in a sour environment. Surf Coating Technol 2020;399.
[17] Jack TA, Pourazizi R, Ohaeri E, Szpunar J, Zhang J, Qu J. Investigation of the hydrogen induced cracking behaviour of API 5L X65 pipeline steel. Int J Hydrogen Energy 2020;45(Issue 35):17671–84.
[18] Fragiel A, Serna S, Malo-Tamayo J, Silva P, Campillo B, Martínez-Martínez E, et al. Effect of microstructure and temperature on the stress corrosion cracking of two microalloyed pipeline steels in H_2S environment for gas transport. Eng Fail Anal 2019;105:1055–68.
[19] Hosseini Far AR, Mousavi Anijdan SH, Abbasi SM. The effect of increasing Cu and Ni on a significant enhancement of mechanical properties of high strength low alloy, low carbon steels of HSLA-100 type. Mater Sci Eng, A 2019;746:384–93.
[20] Mousavi Anijdan SH, Sabzi M. The evolution of microstructure of an high Ni HSLA X100 forged steel slab by thermomechanical controlled processing. TMS Annual Meeting & Exhibition 2018:145–56.
[21] Mousavi Anijdan SH, Yue S. The necessity of dynamic precipitation for the occurrence of no-recrystallization temperature in Nb-microalloyed steel. Mater Sci Eng, A 2011;528:803–7.
[22] Ghosh KS, Mondal DK. Mechanical and electrochemical behavior of a high strength low alloy steel of different grain sizes. Metall Mater Trans 2013;44:3608–22.
[23] Mousavi Anijdan SH, Yue S. The effect of cooling rate, and cool deformation through strain-induced transformation, on microstructural evolution and mechanical properties of microalloyed steels. Metall Mater Trans 2012;43:1140–62.
[24] Mousavi Anijdan SH, Sediako D, Yue S. Optimization of flow stress in cool deformed Nb-microalloyed steel by combining strain induced transformation of retained austenite, cooling rate and heat treatment. Acta Mater 2012;60:1221–9.
[25] Mousavi Anijdan SH, Hoseini M, Yue S. Texture development in cool deformed microalloyed steels. Mater Sci Eng, A 2011;528:6788–93.
[26] Godefroida LB, Senaa BM, Filhoa VBT. Evaluation of microstructure and mechanical properties of seamless steel pipes API 5L, type obtained by different processes of heat treatments. Mater Res 2017;20(2):514–22.
[27] Sabzi M, Mersagh Dezfuli S, Asadian M, Tafi A, Mahaab A. Study of the effect of temperature on corrosion behavior of galvanized steel in seawater environment by using potentiodynamic polarization and EIS methods. Mater Res Express 2019;6(Number 7):1–9.
[28] Sabzi M, Mersagh Dezfuli S. Deposition of Al_2O_3 ceramic film on copper-based heterostructured coatings by aluminizing process: study of the electrochemical responses and corrosion mechanism of the coating .International Journal of Applied Ceramic Technology 2019;16(Issue1):195–210.
[29] Asadian M, Sabzi M, Mousavi Anijdan SH. The effect of temperature, CO_2, H_2S gases and the resultant iron carbonate and iron sulfide compounds on the sour corrosion behaviour of ASTM A-106 steel for pipeline transportation. Int J Pres Ves Pip 2019;171:184–93.
[30] Sabzi M, Jozani AH, Zeidvandi F, Sadeghi M, Dezfuli SM. Effect of 2-Mercaptobenzothiazole concentration on the sour corrosion behavior of API X60 pipeline steel: electrochemical parameters and adsorption mechanism. International Journal of Minerals, Metallurgy and Materials 2020. In press.
[31] Bordbar S, Alizadeh M, Hashemi SH. Effects of microstructure alteration on corrosion behavior of welded joint in API X70 pipeline steel. Mater Des 2013;45:597–604.
[32] Sabzi M, Moeini Far S, Mersagh Dezfuli S. Effect of melting temperature on microstructural evolutions, behavior and corrosion morphology of Hadfield austenitic manganese steel in the casting process. International Journal of Minerals, Metallurgy, and Materials 2018;25(12):1431–8.
[33] Sabzi M, Moeini Far S, Mersagh Dezfuli S. Characterization of bioactivity behavior and corrosion responses of hydroxyapatite-ZnO nanostructured coating deposited on NiTi shape memory alloy. Ceram Int 2018;44:21395–405.
[34] Santos BAF, Serenario MED, Souza RC, Oliveira JR, Vaz GL, Gomes JACP, et al. The electrolyte renewal effect on the corrosion mechanisms of API X65 carbon steel under sweet and sour environments. J Petrol Sci Eng 2021;199:108347.
[35] deOliveira MC, Figueredo RM, Acciari HA, Codaro EN. Corrosion behavior of API 5L X65 steel subject to plastic deformation. Journal of Materials Research and Technology 2018;7(Issue 3):314–8.
[36] Golchinvafa A, Mousavi Anijdan SH, Sabzi M, Sadeghi M. The effect of natural inhibitor concentration of Fumaria officinalis and temperature on corrosion protection mechanism in API X80 pipeline steel in 1 M H_2SO_4 solution. Int J Pres Ves Pip 2020;188:104241.
[37] Mousavi Anijdan SH, Sabzi M, Asadian M, Jafarian HR. Effect of sub-layer temperature during HFCVD process on morphology and corrosion behavior of tungsten carbide coating. Int J Appl Ceram Technol 2019;16:243–53.
[38] Zhang S, Hou L, Du H, Wei H, Liu B, Wei Y. A study on the interaction between chloride ions and CO_2 towards carbon steel corrosion. Corrosion Sci 2020;167:108531.
[39] Tang Y, Guo XP, Zhang GA. Corrosion behaviour of X65 carbon steel in supercritical-CO_2 containing H_2O and O_2 in carbon capture and storage (CCS) technology. Corrosion Sci 2017;118:118–28.
[40] Ohaeri E, et al. Hydrogen induced cracking susceptibility of API 5L X70 pipeline steel in relation to microstructure and crystallographic texture developed after different thermomechanical treatments. Mater Char 2018;145:142–56.
[41] Korda AA, Taufiq T. Hydrogen induced cracking of API X52 and X60 sour service steels subjected to pre-strain under prolonged H_2SExposure. IOP Conf Ser: Mater Sci Eng 2019;547:1–14.
[42] Cotterill P. The hydrogen embrittlement of metals. Prog Mater Sci 1961;9(Issue 4):205–50.
[43] Stalheim Douglas G, Hoh Bernhard. Guidelines for production of API pipelines steels suitable for hydrogen induced cracking (HIC) service applications. Proceedings of the 2010 8th international pipeline conference. 2010 8th

international pipeline conference, vol. 2; 2010. p. 517–27. Calgary, Alberta, Canada. September 27–October 1.
[44] Dong Ch, et al. Hydrogen induced cracking of X80 pipeline steel. International Journal of Minerals, Metallurgy, and Materials 2010;17:579–86.
[45] Bai P, et al. Hydrogen embrittlement of X80 pipeline steel in H2S environment: effect of hydrogen charging time, hydrogen-trapped state and hydrogen charging–releasing–recharging cycles. International Journal of Minerals, Metallurgy and Materials 2020;27:63–73.
[46] Tetelman AS, Robertson WD. The mechanism of hydrogen embrittlement observed in iron silicon single crystal. American Institute of Mining and Metallurgical Engineers 1962;224:775–83.
[47] Zapffe C, Sims CE. Hydrogen embrittlement, internal stress and defects in steel. American Institute of Mining and Metallurgical Engineers 1941;145:225–32.